Optimal design of a T1 super-resolution reconstruction experiment: a simulation study

M. Nicastro[1], Q. Beirinckx[1], P. Bladt[1], B. Jeurissen[1], S. Klein[2], J. Sijbers[1], D.H.J. Poot[2], A.J. den Dekker[1]
[1]imec - Vision Lab, Dept of Physics, University of Antwerp, Antwerp, Belgium
[2]Biomedical Imaging Group Rotterdam, Department of Radiology and Medical Informatics, Erasmus Medical Center, Rotterdam, The Netherlands

Synopsis: Model-based Super Resolution Reconstruction (SRR) methods have recently been applied in MR relaxometry to address the need for an improved trade-off between spatial resolution, precision, and acquisition time. In this work, an optimal experimental design framework is proposed to identify acquisition settings for T1-SRR that maximize the precision of the estimated T1. This optimization is required to exploit the full benefits provided by the SSR methods. The optimized settings were compared to a reference acquisition protocol by means of Monte Carlo simulations.

INTRODUCTION

T1 Super-Resolution Reconstruction (T1-SRR) method aims to reconstruct a high-resolution (HR) 3-D isotropic T1 parametric map from a set of multi-slice anisotropic inversion recovery turbo spin echo T1-weighted images with a low through-plane resolution acquired with different slice orientations around the phase-encoding axis. The optimal experimental design framework proposed in this work is based on the Cramér-Rao lower bound (CRLB) [2-4] and identifies acquisition settings for T1-SRR that maximize the T1 estimation precision. The optimized settings are compared to a reference acquisition protocol by means of Monte Carlo simulations. This study presents a step toward protocol standardization of quantitative SRR.

METHODS

CRLB and T1-SRR model: The cost function of the experiment design is based on the CRLB, which is a lower bound on the variance of unbiased estimators and which is given by the inverse of the Fisher Information Matrix (FIM). The FIM $\boldsymbol{J}$ of the T1-SRR model, assuming Gaussian white noise with standard deviation σ is given by:

$$\mathbf{J} = \frac{1}{\sigma^2}\sum_{m=1}^{M}\frac{\partial \boldsymbol{s}_m^T}{\partial \boldsymbol{\theta}}\frac{\partial \boldsymbol{s}_m}{\partial \boldsymbol{\theta}^T} \qquad \frac{\partial \boldsymbol{s}_m}{\partial \boldsymbol{\theta}^T} = \left[\frac{\partial \boldsymbol{s}_m}{\partial \boldsymbol{\rho}^T}, \frac{\partial \boldsymbol{s}_m}{\partial \boldsymbol{T1}^T}\right]$$

$$\frac{\partial \boldsymbol{s}_m}{\partial \boldsymbol{\rho}^T} = diag\big(sgn(\boldsymbol{s}_m)\big)\overline{\boldsymbol{D}}\boldsymbol{G}(\alpha_m)diag\left(\frac{\partial \boldsymbol{r}(TI_m)}{\partial \rho}\right) \qquad \frac{\partial \boldsymbol{s}_m}{\partial \boldsymbol{T1}^T} = diag\big(sgn(\boldsymbol{s}_m)\big)\overline{\boldsymbol{D}}\boldsymbol{G}(\alpha_m)diag\left(\frac{\partial \boldsymbol{r}(TI_m)}{\partial T1}\right)$$

where $\boldsymbol{T1} \in \mathbb{R}^{N_r \times 1}$, $\boldsymbol{\rho} \in \mathbb{R}^{N_r \times 1}$, $\boldsymbol{s}_m \in \mathbb{R}^{N_s \times 1}$ and $\boldsymbol{r}(TI_m) \in \mathbb{R}^{N_r \times 1}$ are the T1 and proton density map to be estimated, the m-th low resolution (LR) magnitude 2D T1-weighted image and the 2D high-resolution (HR) T1-weighted image (with inversion time TI_m) defined as in [1], with N_r and N_s the number of voxels of the HR and LR 2D images, respectively, and M the number of acquired LR 2D T1-w images. The linear operator $\overline{\boldsymbol{D}}$ describes blurring and down-sampling by averaging along the through-plane direction. The linear operator $\boldsymbol{G}(\alpha_m)$ describes the rotation of the acquisition plane over angle α_m for the m-th LR T1-w image, which was implemented as in [5].

Optimal Experimental Design Framework: A cost function based on the sum of the coefficients of variation of the T1 parameters derived from the CRLBs is minimized with regard to the acquisition settings $\boldsymbol{Q} = [\boldsymbol{TI}, \boldsymbol{\alpha}]$:

$$\widehat{\boldsymbol{Q}} = arg\min_{\boldsymbol{Q}} \sum_{i=N_r+1}^{2N_r} (J^{-1})_{ii}/T1_{i-N_r}^2$$

where $\boldsymbol{Q}$, $\widehat{\boldsymbol{Q}} \in \mathbb{R}^{2M \times 1}$ and $(J^{-1})_{ii}$ represents the i-th diagonal element of the CRLB matrix J^{-1}.

Proof-of-concept experiment: The translational symmetry of the 3D SRR problem along the phase encoding direction has been exploited to evaluate the T1-SSR framework in 2D, reducing computational complexity and memory consumption. $\rho, T1$ ground truth maps of size 64 x 64 have been simulated from an anatomical model of a manually masked 2D brain sagittal slice [6,7] (Fig. 1). The framework was used to improve the acquisition setup proposed by [1], based on M=14 LR images acquired with an anisotropy factor (AF) of 2.67.

Optimization strategy: To solve the optimization problem, first the value of the cost function was evaluated in 1000 random points $\boldsymbol{Q}$ in the domains [50, 3000] ms and [0, 180]° for TI and α, respectively. Subsequently, a constrained iterative minimization method ('interior-point' algorithm) was started at the point with the lowest cost. The optimization was halted after 1000 cost function evaluations in order to approach a minimum in a feasible computation time.

Monte Carlo simulation: A Maximum Likelihood Estimator (MLE) framework similarly to [1] was implemented where the regularization terms were set to zero. 50 noise realizations (σ = 0.02, SNR=50) were simulated for each acquisition setup. RMSE maps for the two setups were computed to compare the setups in terms of accuracy and precision.

RESULTS

The rotation angles and TIs for the optimized and reference designs are reported in Table 1. The square root CRLB maps for the two setups and the RMSE maps computed from the Monte Carlo simulations are shown in Fig. 2 and Fig. 3, respectively.

DISCUSSION

In the optimized setup, contrary to the reference setup, the rotation angles and TIs are no longer uniformly/log-uniformly distributed**.** The optimized TIs appear clustered around distinct values, in line with the finding of Karlsen et al. [8] in the context of optimal design for T1 mapping without SSR.

From the CRLB maps, we can observe that the increase in T1 estimation precision came at the cost of a reduced ρ estimation precision, coherently with our minimization problem definition. The RMSE maps confirms the predictions of the CRLB map, showing a reduced error in particular in the T1 CSF quantification. It is worth to notice that, in this preliminary study, the optimization procedure was limited to a single brain slice. A future step will be to include prior information from a variety of brain anatomies in order to improve generalizability.

CONCLUSION

Quantitative SRR methods are a topic of interest for an increasing number of researchers for their promising but still uncovered potential. Studies aimed at method standardization are thus becoming a need. In this frame, a proof-of-concept statistical optimal experimental design framework was proposed and successfully applied to T1-SRR in a limited study case. Future studies will be addressed to the extension of the framework for more general applicability.

REFERENCES

1. Van Steenkiste, G., Poot, D., Jeurissen, B., den Dekker, A., Vanhevel, F., Parizel, P., and Sijbers, J. (2016). Super-resolution T1 estimation: Quantitative high-resolution T1 mapping from a set of low-resolution T1-weighted images with different slice orientations. Magnetic Resonance in Medicine, 77(5), pp.1818-1830. https://doi.org/10.1002/mrm.26262
2. V.V. Fedorov. Theory of Optimal Experiments. New York: Academic Press, 1972.
3. A.C. Atkinson and A.N. Donev. Optimum Experimental Designs. Oxford: Clarendon, 1992.
4. A. van den Bos, Parameter estimation for scientists and engineers. https://onlinelibrary.wiley.com/doi/book/10.1002/9780470173862
5. Larkin KG, Oldfield MA, Klemm H. Fast Fourier method for the accurate rotation of sampled images. Opt. Commun., 1997. 139(1-3):99–106. https://doi.org/10.1016/S0030-4018(97)00097-7
6. Cocosco CA, Kollokian V, Kwan RKS, Evans AC. BrainWeb: online interface to a 3D MRI simulated brain database. Neuroimage 1997;5: S425.
7. Gold, G. E., Han, E., Stainsby, J., Wright, G., Brittain, J., & Beaulieu, C. (2004). Musculoskeletal MRI at 3.0 T: Relaxation Times and Image Contrast. American Journal of Roentgenology, 183(2), 343–351. https://doi.org/10.2214/ajr.183.2.1830343

Acknowledgments / Funding Information: This research was conducted as part of the B-Q MINDED project which received funding from the European Union's Horizon 2020 research and innovation programme under the Marie Skłodowska-Curie grant agreement No 764513.

Table 1

Reference Setup		Optimized Setup	
α_m (°)	Ti_m (ms)	α_m (°)	Ti_m (ms)
0	100	15.6	554
25.7	130	62.8	565
51.4	169	45.7	631
77.1	219	164.7	658
102.8	285	134.1	663
128.5	370	107.4	700
154.2	481	138.5	737
0	624	41.99	1934
25.7	811	152	2881
51.4	1054	135.8	2896
77.1	1369	109.8	2923
102.8	1778	7.2	2935
128.5	2309	72.8	2947
154.2	3000	47.4	2988

Table 1: Rotation angles and TI values for the reference and optimized acquisition setups, sorted by TI values: The reference set proposed by [1] consists of seven subsets, each simulated with a different slice orientation and each acquired with two TIs. The optimized setup is the final output of the optimal experimental design method.

Figure 1

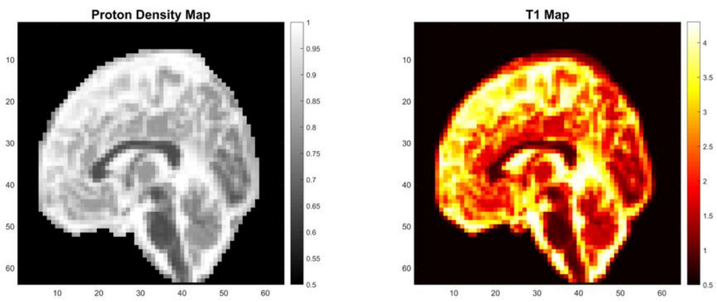

Figure 1: Ground Truth Proton Density (ρ) and T1 Maps. A sagittal brain slice simulated from an 11-compartments anatomical model of BrainWeb Database [6] using the typical ρ and T1 values at 3T [7], manually masked.

Figure 2

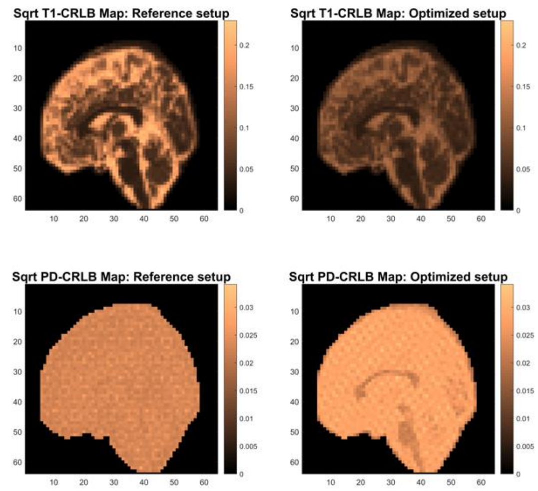

Figure 2: Square root CRLB Maps for the reference and optimized acquisition setups. The square root CRLB maps were obtained by extracting the square roots of the diagonal elements of the CRLB matrix and mapping them to the original reference image size. The optimized setup shows a reduction of the T1-CRLB map values. which reflects an increase in the achievable precision of the estimated T1 map compared with the reference setup.

Figure 3

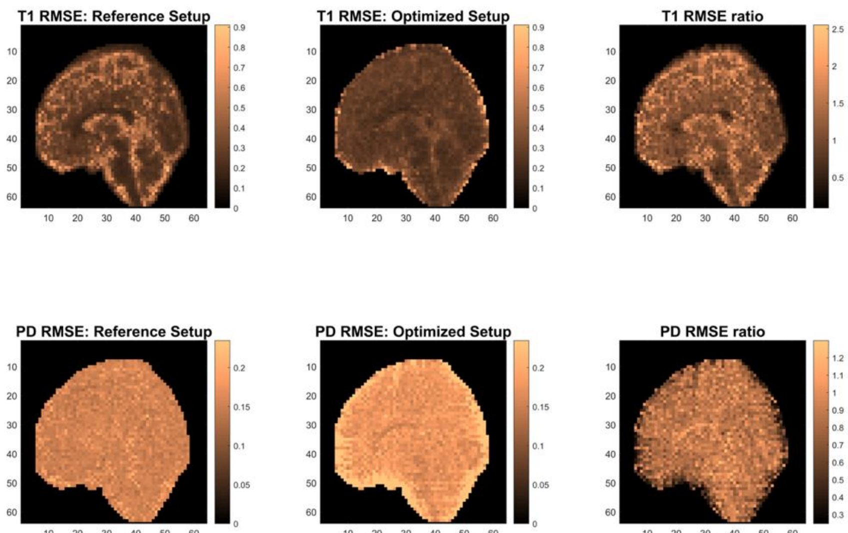

Figure 3: RMSE Maps from the Monte Carlo experiment. The rows show the RMSE computed for the reference setup, the optimized setup, and the ratio between the RMSE for the reference and optimized setup, respectively, for T1 (top row) and proton density (bottom row).